Characterization of the noise effect on weak synchronization

Sang-Yoon Kim,[1,2] Woochang Lim,[1] Alexei Jalnine,[3] and Sergey P. Kuznetsov[3,4]
[1]*Department of Physics, Kangwon National University, Chunchon, Kangwon-Do 200-701, Korea*
[2]*Institute for Research in Electronics and Applied Physics, University of Maryland, College Park, Maryland 20742*
[3]*Department of Nonlinear Processes, Saratov State University, Astrkhanskaya Street 83, Saratov 410026, Russia*
[4]*Institute of Radio-Engineering and Electronics, Russian Academy of Sciences, Zelenaya 38, Saratov 410019, Russia*
(Received 7 June 2002; published 30 January 2003)

We investigate the noise effect on weak synchronization in two coupled identical one-dimensional (1D) maps. Due to the existence of positive local transverse Lyapunov exponents, the weakly stable synchronous chaotic attractor (SCA) becomes sensitive with respect to the variation of noise intensity. To quantitatively characterize such noise sensitivity, we introduce a quantifier, called the noise sensitivity exponent (NSE). For the case of bounded noise, the values of the NSE are found to be the same as those of the exponent characterizing a parameter sensitivity of the weakly stable SCA in presence of a parameter mismatch between the two 1D maps. Furthermore, it is found that the scaling exponent for the average time spent near the diagonal for both the bubbling and riddling cases occurring in the regime of weak synchronization is given by the reciprocal of the NSE, as in the parameter-mismatching case. Consequently, both the noise and parameter mismatch have the same effect on the scaling behavior of the average characteristic time.

DOI: 10.1103/PhysRevE.67.016217 PACS number(s): 05.45.Xt

I. INTRODUCTION

Recently, the phenomenon of synchronization in coupled chaotic systems has become a field of intensive study. For this case of chaos synchronization, a synchronous chaotic motion occurs on an invariant subspace of the whole phase space [1–4]. Particularly, this type of chaos synchronization has attracted much attention, because of its potential practical application in secure communication [5].

If a synchronous chaotic attractor (SCA) on the invariant subspace is stable against a perturbation transverse to the invariant subspace, it may become an attractor in the whole phase space. Properties of transverse stability of the SCA are intimately associated with transverse bifurcations of unstable periodic orbits embedded in the SCA [6–12]. If all such unstable periodic orbits are transversely stable, the SCA becomes asymptotically stable, and hence we have ''strong'' synchronization. However, as the coupling parameter passes through a threshold value, an unstable periodic orbit first becomes transversely unstable through a local bifurcation. After this first transverse bifurcation, trajectories may be locally repelled from the invariant subspace when they visit the neighborhood of the transversely unstable periodic orbit point. Thus, loss of strong synchronization begins with such a first transverse bifurcation, and then we have ''weak'' synchronization. For this case, intermittent bursting or basin riddling may occur depending on the existence of an absorbing area, controlling the global dynamics, inside the basin of attraction [10–13]. In the presence of an absorbing area, acting as a bounded trapping vessel, locally repelled trajectories from the invariant subspace are restricted to move within the absorbing area, and exhibit transient intermittent bursting from the invariant subspace [14,15]. On the other hand, in the absence of such an absorbing area, the locally repelled trajectories will go to another attractor (or infinity), and hence the basin of attraction becomes riddled with a dense set of repelling ''holes,'' belonging to the basin of another attractor (or infinity) [16].

However, in a real situation a small noise and a small mismatch between the subsystems are unavoidable. Hence the effect of noise and parameter mismatching must be taken into consideration for the study on the loss of chaos synchronization. In the regime of weak synchronization, transversely unstable periodic orbits are embedded in the SCA. Hence, when a typical trajectory visits the neighborhoods of such unstable periodic orbits, it experiences local transverse repulsion from the diagonal. As a result, the typical trajectory may have segments exhibiting positive local (finite time) transverse Lyapunov exponents, even if the averaged transverse Lyapunov exponent is negative. Because of the existence of these positive local transverse Lyapunov exponents, the weakly stable SCA becomes sensitive with respect to the variation of the noise intensity and mismatching parameter. This is in contrast to the case of the strong synchronization that has no such sensitivity. Note also that, due to the existence of positive local Lyapunov exponents, strange nonchaotic attractors that appear typically in quasiperiodically forced systems exhibit a sensitivity with respect to the phase of the quasiperiodic force. Such phase sensitivity was characterized quantitatively in terms of the phase sensitivity exponent [17]. In a similar way, two of us (Jalnine and Kim) introduced the parameter sensitivity exponent, and quantitatively characterized the degree of the parameter sensitivity of the weakly stable SCA [18].

In this paper we investigate the effect of bounded noise on weak synchronization in two coupled identical one-dimensional (1D) maps with an invariant diagonal. To quantitatively characterize the noise sensitivity of the weakly stable SCA, we introduce a quantifier, called the noise sensitivity exponent (NSE), in Sec. II. Thus the NSE that measures the degree of the noise sensitivity becomes a quantitative characteristic of the weakly stable SCA. As the coupling parameter c is varied away from the point of the first

transverse bifurcation, successive transverse bifurcations of periodic saddles embedded in the SCA occur. Hence the value of the NSE increases because local transverse repulsion of the embedded periodic repellers becomes more and more strong, and it tends to infinity as c approaches the blow-out bifurcation point where the averaged transverse Lyapunov exponent becomes zero. As a result of this blow-out bifurcation, the weakly stable SCA becomes transversely unstable [19]. Furthermore, the values of the NSE are found to become the same as those of the parameter sensitivity exponent, because their values are determined only by the (same) local transverse Lyapunov exponents of the weakly stable SCA. In the presence of noise, the weakly stable SCA is replaced by a bubbling attractor or a chaotic transient. In both cases, the quantity of interest is the average time spent near the diagonal (i.e., the average interburst time and the average chaotic transient lifetime) [15]. In terms of the NSE, the noise effect on the power-law scaling behavior of such average characteristic time τ is characterized in Sec. III. As the NSE increases, local transverse repulsion of the periodic repellers embedded in the SCA becomes strong, and hence τ becomes short. It is thus found that the scaling exponent for τ and the NSE has a reciprocal relation, as in the parameter-mismatching case [18]. Hence the noise and parameter mismatch have essentially the same effect on the power-law scaling behavior of τ. Finally, we give a summary in Sec. IV.

II. CHARACTERIZATION OF THE NOISE SENSITIVITY

In this section, we study the effect of additive and parametric noise on the weakly stable SCA. For the case of weak synchronization, the SCA becomes sensitive with respect to the variation of noise strength. We introduce a quantifier, called the NSE, and quantitatively characterize the noise sensitivity of the weakly stable SCA. It is thus found that the values of the NSE become the same as those of the parameter sensitivity exponent, independently of whether the noise is additive or parametric.

We first investigate the effect of additive noise on weak synchronization in two coupled identical 1D maps [12]

$$T:\begin{cases} x_{n+1}=F(x_n,y_n)=f(x_n,a)+(1-\alpha)cg(x_n,y_n)+\sigma\xi_n^{(1)} \\ y_{n+1}=G(x_n,y_n)=f(y_n,a)+c\,g(y_n,x_n)+\sigma\xi_n^{(2)}, \end{cases} \tag{1}$$

where x_n and y_n are state variables of the subsystems at a discrete time n, local dynamics in each subsystem with a control parameter a is governed by the 1D map $f(x,a)=1-ax^2$, c is a coupling parameter between the two subsystems, and $g(x,y)$ is a coupling function of the form

$$g(x,y)=y^2-x^2. \tag{2}$$

For $\alpha=0$, the coupling becomes symmetric, while for nonzero α $(0<\alpha\leqslant 1)$ it becomes asymmetric. The extreme case of asymmetric coupling with $\alpha=1$ corresponds to the unidirectional coupling. In such a way, α tunes the degree of asymmetry in the coupling. In an ideal case without noise (i.e., $\sigma=0$), there exists an invariant synchronization line, $y=x$, in the $(x-y)$ phase space. However, in a real situation noise is unavoidable, and hence the diagonal is no longer invariant. To take into consideration such noise effect, random numbers are added to Eq. (1). For this case $\xi_n^{(i)}$ $(i=1,2)$ are statistically independent random numbers chosen at each discrete time n from the uniform distribution with a zero mean $\langle\xi_n^{(i)}\rangle=0$ and a unit variance $\langle\xi_n^{(i)2}\rangle=1$. Hence $\xi_n^{(i)}$ are just bounded random values uniformly distributed in the interval $[-\sqrt{3},\sqrt{3}]$, and σ controls the "strength" of such a random noise.

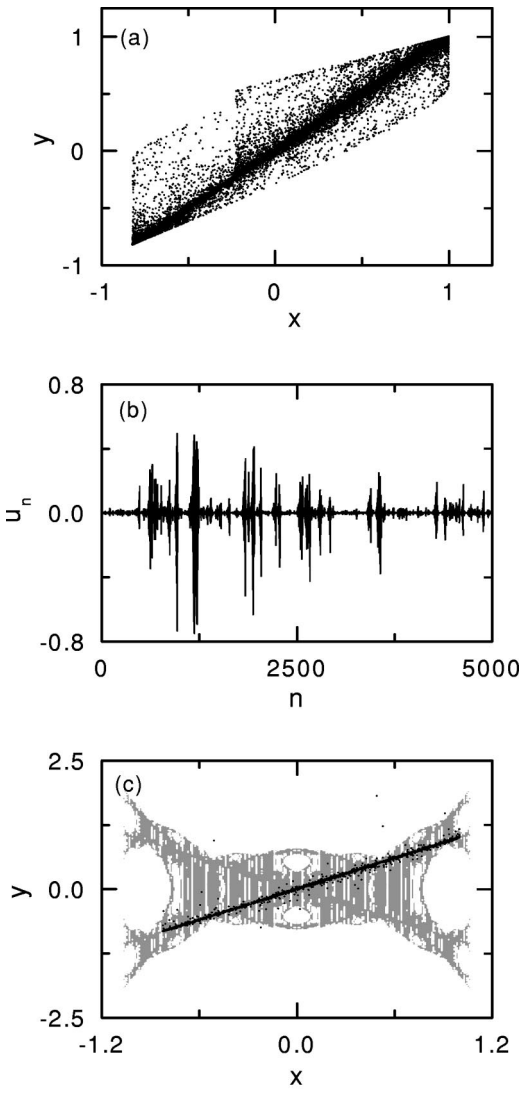

FIG. 1. Effect of the additive noise with $\sigma=0.0005$ on weak synchronization for $a=1.82$ in the unidirectionally coupled case of $\alpha=1$. (a) A bubbling attractor and (b) the evolution of the transverse variable u_n $(=x_n-y_n)$ representing the deviation from the diagonal versus n for the bubbling case of $c=-0.7$. For the riddling case of $c=-2.91$ the SCA with a basin (gray region) riddled with a dense set of repelling "holes" leading to divergent orbits (white region) for $\sigma=0$ is transformed into a chaotic transient (black dots) for $\sigma=0.0005$ as shown in (c). The sequence of $\{u_n\}$ in (b) and the chaotic transient in (c) are obtained from the trajectories starting from the same initial point $(x_0^*,y_0^*)=(0.5,0.5)$.

As an example, we choose the unidirectionally coupled

case of $\alpha=1$ [11]. For this case, the drive 1D map acts on the response 1D map, while the response 1D map does not influence the drive one. Here we fix the value of a as $a=1.82$, and investigate the noise effect by varying the coupling parameter c. For this case an SCA exists in the interval of $c_{b,l}[\simeq -2.963]<c<c_{b,r}[\simeq -0.677]$. As the coupling parameter c passes $c_{b,l}$ or $c_{b,r}$, the SCA loses its transverse stability through a blow-out bifurcation, and then a complete desynchronization occurs. In the regime of synchronization, a strongly stable SCA exists for $c_{t,l}[\simeq -2.789]<c<c_{t,r}[\simeq -0.850]$. For this case of strong synchronization, the SCA exhibits no noise sensitivity, because all periodic saddles embedded in the SCA are transversely stable. However, as the coupling parameter c passes $c_{t,r}$ and $c_{t,l}$, bubbling and riddling transitions occur through the first transverse bifurcations of periodic saddles, respectively, Ref. [11] and then we have weak synchronization. For this case, the weakly stable SCA exhibits a noise sensitivity, because of local transverse repulsion of the periodic repellers embedded in the SCA. Hence, however, small the noise strength σ, a persistent intermittent bursting, called the attractor bubbling, occurs in the regime of bubbling ($c_{t,r}<c<c_{b,r}$). Figures 1(a) and 1(b) show such attractor bubbling for $\sigma=0.0005$. On the other hand, in the regime of riddling ($c_{b,l}<c<c_{t,l}$), the weakly stable SCA with a riddled basin for $\sigma=0$ is transformed into a chaotic transient (denoted by black dots) with a finite lifetime in the presence of noise, as shown in Fig. 1(c). As c is changed away from $c_{t,l}$ or $c_{t,r}$, transversely unstable periodic repellers appear successively in the SCA via transverse bifurcations. Then the degree of the noise sensitivity of the SCA increases, because of the increase in the strength of local transverse repulsion of the periodic repellers embedded in the SCA.

To quantitatively characterize the noise sensitivity of the SCA, we consider an orbit $\{(x_n,y_n)\}$ starting from an initial point on the diagonal (i.e., $x_0=y_0$). As the strength of the local transverse repulsion from the diagonal increases, the SCA becomes more and more sensitive with respect to the variation of σ. Such noise sensitivity of the SCA for $\sigma=0$ may be characterized by calculating the derivative of the transverse variable u_n $(=x_n-y_n)$, denoting the deviation from the diagonal, with respect to σ,

$$\left.\frac{\partial u_{n+1}}{\partial\sigma}\right|_{\sigma=0}=\left.\frac{\partial x_{n+1}}{\partial\sigma}\right|_{\sigma=0}-\left.\frac{\partial y_{n+1}}{\partial\sigma}\right|_{\sigma=0}=\left[\left.\frac{\partial F(x_n,y_n)}{\partial x_n}\right|_{\sigma=0}-\left.\frac{\partial G(x_n,y_n)}{\partial x_n}\right|_{\sigma=0}\right]\left.\frac{\partial x_n}{\partial\sigma}\right|_{\sigma=0}+\left[\left.\frac{\partial F(x_n,y_n)}{\partial y_n}\right|_{\sigma=0}-\left.\frac{\partial G(x_n,y_n)}{\partial y_n}\right|_{\sigma=0}\right]\left.\frac{\partial y_n}{\partial\sigma}\right|_{\sigma=0}+[\xi_n^{(1)}-\xi_n^{(2)}]. \tag{3}$$

Using Eq. (1), we obtain the following recurrence relation

$$\left.\frac{\partial u_{n+1}}{\partial\sigma}\right|_{\sigma=0}=[f_x(x_n^*,a)-(2-\alpha)ch(x_n^*)]\left.\frac{\partial u_n}{\partial\sigma}\right|_{\sigma=0}+[\xi_n^{(1)}-\xi_n^{(2)}], \tag{4}$$

where f_x is the derivative of f with respect to x, $\{(x_n^*,y_n^*)\}$ is the synchronous orbit with $x_n^*=y_n^*$ for $\sigma=0$, and $h(x)$ is a reduced coupling function defined by $h(x)\equiv\partial g(x,y)/\partial y|_{y=x}$ [20]. Iterating the formula (4) along a synchronous trajectory starting from an initial point (x_0^*,y_0^*) on the diagonal, we may obtain derivatives at all subsequent points of the trajectory:

$$\left.\frac{\partial u_N}{\partial\sigma}\right|_{\sigma=0}=\sum_{k=1}^{N}R_{N-k}(x_k^*)[\xi_{k-1}^{(1)}-\xi_{k-1}^{(2)}]+R_N(x_0^*)\left.\frac{\partial u_0}{\partial\sigma}\right|_{\sigma=0}, \tag{5}$$

where

$$R_M(x_m^*)=\prod_{i=0}^{M-1}[f_x(x_{m+i}^*,a)-(2-\alpha)ch(x_{m+i}^*)] \tag{6}$$

and $R_0=1$. Note that the factor $R_M(x_m^*)$ is associated with a local (M-time) transverse Lyapunov exponent $\sigma_M^T(x_m^*)$ of the SCA that is averaged over M synchronous orbit points starting from x_m^* as follows:

$$\sigma_M^T(x_m^*)=\frac{1}{M}\ln|R_M(x_m^*)|. \tag{7}$$

Thus $R_M(x_m^*)$ becomes a local (transverse stability) multiplier that determines local sensitivity of the transverse motion during a finite time M. As $M\to\infty$, σ_M^T approaches the usual transverse Lyapunov exponent σ_T that denotes the average exponential rate of divergence of an infinitesimal perturbation transverse to the SCA. If we introduce a new random variable $\eta_n=\xi_n^{(1)}-\xi_n^{(2)}$, Eq. (5) reduces to

$$\left.\frac{\partial u_N}{\partial\sigma}\right|_{\sigma=0}=S_N^{(n)}(x_0^*)\equiv\sum_{k=1}^{N}R_{N-k}(x_k^*)\,\eta_{k-1}, \tag{8}$$

because $\partial u_0/\partial\sigma|_{\sigma=0}=0$. Here η_n are bounded random numbers distributed in the interval $[-2\sqrt{3},2\sqrt{3}]$, and their distribution density function will be given below.

For the case of weak synchronization, transversely unstable periodic repellers are embedded in the SCA. When a typical trajectory visits neighborhoods of such repellers and their preimages, it has segments experiencing local repulsion from the diagonal. Consequently, the distribution of local transverse Lyapunov exponents σ_M^T for a large ensemble of trajectories and large M may have a positive tail [see Fig. 5 in Ref. [18]]. For the segments of a trajectory exhibiting a positive local transverse Lyapunov exponent ($\sigma_M^T>0$), the local multipliers R_M $[=\pm\exp(\sigma_M^T M)]$ can be arbitrarily large, and hence the partial sum $S_N^{(n)}$ may be arbitrarily large. This implies the unbounded growth of the derivatives $\partial u_N/\partial\sigma|_{\sigma=0}$ as N tends to infinity. Consequently, the weakly stable SCA may exhibit a noise sensitivity. As an example,

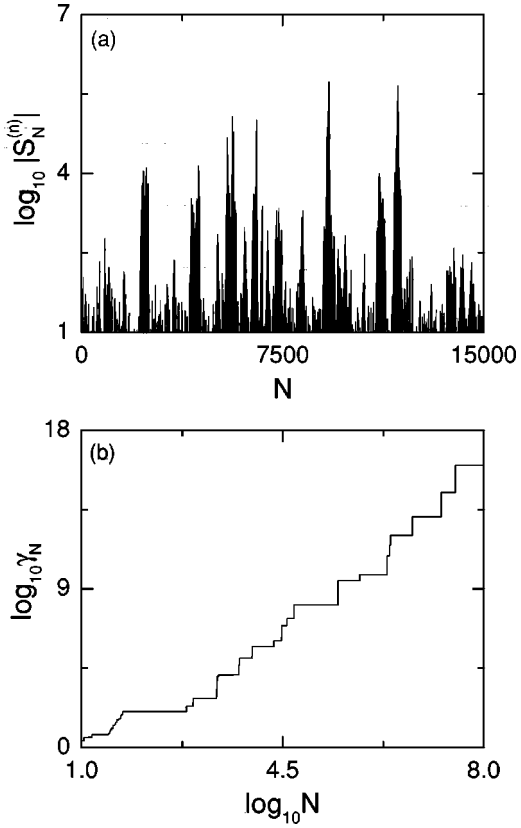

FIG. 2. (a) Intermittent behavior of the partial sum $|S_N^{(n)}|$ for $\alpha=1$, $a=1.82$, and $c=-0.7$. (b) The function γ_N looking only at the maximum of $|S_N^{(n)}|$. Note that γ_N grows unboundedly with N. The results in (a) and (b) are obtained from the trajectory starting from the initial orbit point $(x_0^*, y_0^*)=(0.5,0.5)$.

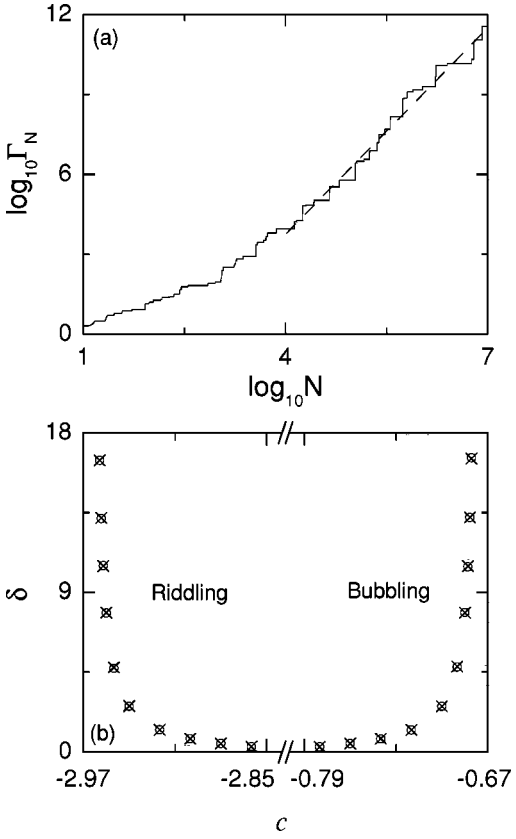

FIG. 3. (a) Noise sensitivity function Γ_N for $\alpha=1$, $a=1.82$, and $c=-0.7$ that takes the minimum value of γ_N in the ensemble containing 100 randomly chosen initial orbit points on the diagonal. It is well fitted with a dashed line with slope $\delta\simeq 2.58$. (b) Plot of the NSEs δ (denoted by the open circles) versus c for the bubbling and riddling cases for $\alpha=1$ and $a=1.82$. Note that the values of the NSEs are the same as those of the parameter sensitivity exponent (denoted by the crosses) within the numerical accuracy.

we consider the case of weak synchronization for $c=-0.7$. If we iterate Eqs. (1) and (4) starting from an initial orbit point (x_0^*, y_0^*) on the diagonal and $\partial u_0/\partial\sigma|_{\sigma=0}=0$, then we obtain the partial sum $S_N^{(n)}(x_0^*)$ of Eq. (8). The results of such calculation for a trajectory starting from $(x_0^*, y_0^*)=(0.5,0.5)$ are presented in Fig. 2(a). The quantity $S_N^{(n)}$ seems very intermittent. However, looking only at the maximum

$$\gamma_N(x_0^*)=\max_{0\le k\le N}|S_k^{(n)}(x_0^*)|, \tag{9}$$

one can easily see the boundedness of $S_N^{(n)}$. Figure 2(b) shows such function γ_N. Note that γ_N grows unboundedly and exhibits no saturation. Consequently, the weakly stable SCA exhibits a noise sensitivity. This is in contrast to the case of strong synchronization for which the SCA has no noise sensitivity because the function γ_N saturates with N.

The growth rate of the function $\gamma_N(x_0^*)$ with time N represents a degree of the noise sensitivity, and can be used as a quantitative characteristic of the weakly stable SCA. However, $\gamma_N(x_0^*)$ depends on a particular trajectory. To obtain a representative quantity, we consider an ensemble of initial points randomly chosen with uniform probability in the range of $x\in(1-a,1)$ on the diagonal, and take the minimum value of γ_N with respect to the initial orbit points,

$$\Gamma_N=\min_{x_0^*}\gamma_N(x_0^*). \tag{10}$$

Figure 3(a) shows a noise sensitivity function Γ_N for $c=-0.7$. Note that Γ_N grows unboundedly with some power δ,

$$\Gamma_N\simeq N^{\delta}. \tag{11}$$

Here the value $\delta\simeq 2.58$ is a quantitative characteristic of the noise sensitivity of the SCA, and we call it as NSE. In each regime of bubbling or riddling, we obtain the NSEs by changing the coupling parameter c from the bubbling or riddling transition point to the blow-out bifurcation point. For obtaining a satisfactory statistics, we also consider 100 ensembles for each c, each of which contains 100 initial orbit points randomly chosen with uniform probability in the range of $x\in(1-a,1)$ on the diagonal and choose the average value of the 100 NSEs obtained in the 100 ensembles. Figure 3(b) shows the plot of such NSEs (denoted by circles) versus c. Note that the NSE δ monotonically increases as c is

varied away from the bubbling or riddling transition point, and tends to infinity as c approaches the blow-out bifurcation point. This increase in the noise sensitivity of the SCA is caused by the increase in the strength of local transverse repulsion of periodic repellers embedded in the SCA. After the blow-out bifurcation, the weakly stable SCA is transformed into a transversely unstable chaotic saddle exhibiting an exponential noise sensitivity. Thus a complete desynchronization occurs.

We now compare the formula (8) for the partial sum $S_N^{(n)}$ with the following analogous formula for $S_N^{(p)}$ that has been obtained in the parameter-mismatching case [18]:

$$\left.\frac{\partial u_N}{\partial \epsilon}\right|_{\epsilon=0} = S_N^{(p)}(x_0^*) \equiv \sum_{k=1}^{N} R_{N-k}(x_k^*) f_a(x_{k-1}^*, a), \quad (12)$$

where ϵ is a mismatching parameter, f_a is the derivative of $f(x,a)$ with respect to a, and R_{N-k} are local multipliers of Eq. (6). As in the case of noise, the weakly stable SCA exhibits a parameter sensitivity because of the unbounded growth of the partial sum $S_N^{(p)}$ with N. For each case of the noise and parameter mismatch, $S_N^{(n,p)}$ represents the sum of the (same) local multipliers R_{N-k}, multiplied by some coefficients. For the case of noise, the coefficients η_{k-1} are random numbers chosen from the bounded distribution density function, $P(\eta) = -\frac{1}{12}|\eta| + \sqrt{3}/6$, in the interval $[-2\sqrt{3}, 2\sqrt{3}]$ [see Fig. 4(a)], which can be easily obtained using the uniform distribution density functions in the interval $[-\sqrt{3}, \sqrt{3}]$ for the random variables ξ_1 and ξ_2. Since the random numbers η_n are bounded, the boundedness of the partial sum $S_N^{(n)}$ is determined just by the local multipliers R_M. For the case of parameter mismatch, the coefficients are the derivative values $f_a(x_{k-1}^*, a)$ $(= -x_{k-1}^{*2})$. Since the synchronous trajectory $\{x_n^*\}$ on the diagonal is chaotic, the coefficients f_a may be regarded as "weakly correlated" random numbers. Using a histogram method, we obtain the distribution density function for f_a, which is shown in Fig. 4(b). Since the values of f_a are bounded in the interval $[-1,0]$, the boundedness of the partial sum $S_N^{(p)}$ is also determined only by the (same) local multipliers R_M, as in the case of noise. This implies that the noise sensitivity function Γ_N grows unboundedly with the same power as in the case of parameter mismatch. Hence the values of the NSE (denoted by circles) become the same as those of the parameter sensitivity exponent (denoted by crosses), as shown in Fig. 3(b). Note that this is a general result valid for any case of bounded noise.

In addition to the case of additive noise, we also consider the case where the nonlinearity parameters of the 1D maps have small random variations due to external noise. These parametric fluctuations can be simulated by modulating the values of the nonlinearity parameters by uniform random numbers in a small interval. Thus we investigate the effect of such parametric noise on weak synchronization in the following two coupled 1D maps:

$$T: \begin{cases} x_{n+1} = f(x_n, a + \sigma\xi_n^{(1)}) + (1-\alpha)cg(x_n, y_n), \\ y_{n+1} = f(y_n, a + \sigma\xi_n^{(2)}) + cg(y_n, x_n). \end{cases} \quad (13)$$

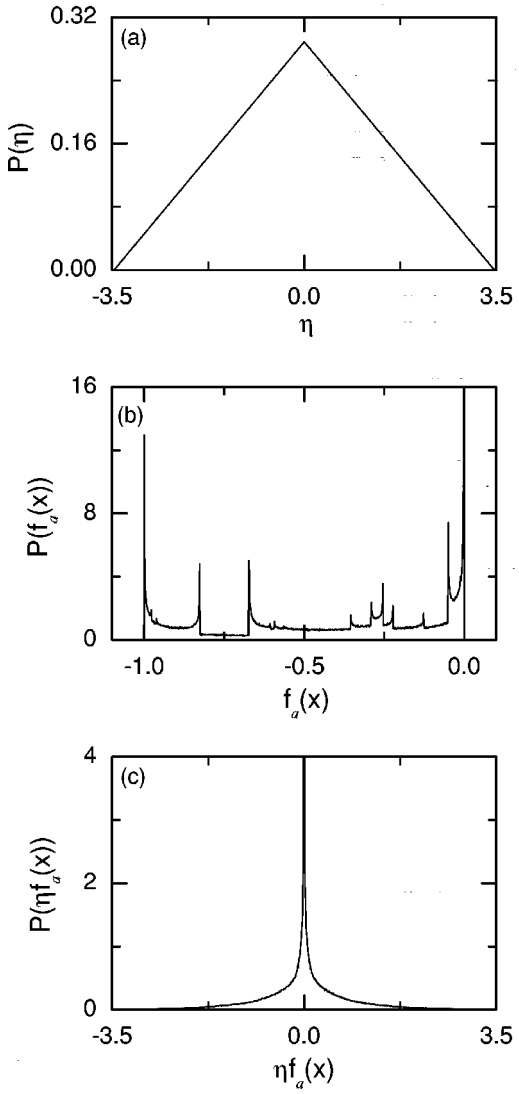

FIG. 4. (a) Distribution density function $P(\eta)$ $(= -\frac{1}{12}|\eta| + (\sqrt{3}/6))$ for the random variable η $(= \xi^{(1)} - \xi^{(2)})$. (b) and (c) Distribution density functions for the variables $f_a(x)$ $(= -x^2)$ and $\eta f_a(x)$ in the case of $\alpha = 1$ and $a = 1.82$. For these cases, the distribution density functions are obtained using a histogram method as follows. We divide each interval ($[-1,0]$ for the case (b) and $[-2\sqrt{3}, 2\sqrt{3}]$ for the case of (c)) into 1000 bins, and get the distribution density from the data of 10^6 orbit points.

Here $\xi^{(1)}$ and $\xi^{(2)}$ are bounded random numbers chosen from the uniform distribution with a zero mean and a unit variance, and σ represents the amplitude of noise. Following the same procedure as in the case of additive noise, one can easily obtain the following recurrence relation for the derivative of the transverse variable u_n $(= x_n - y_n)$ with respect to the noise strength σ,

$$\left.\frac{\partial u_{n+1}}{\partial \sigma}\right|_{\sigma=0} = [f_x(x_n^*, a) - (2-\alpha)ch(x_n^*)] \left.\frac{\partial u_n}{\partial \sigma}\right|_{\sigma=0} + f_a(x_n^*, a)[\xi_n^{(1)} - \xi_n^{(2)}]. \quad (14)$$

Iterating the above formula along the synchronous trajectory

starting from an initial point (x_0^*, y_0^*) on the diagonal, we obtain the derivatives at all points of the trajectory,

$$\left.\frac{\partial u_N}{\partial \sigma}\right|_{\sigma=0} = S_N^{(n)}(x_0^*) \equiv \sum_{k=1}^{N} R_{N-k}(x_k^*)\, \eta_{k-1} f_a(x_{k-1}^*, a), \tag{15}$$

where $\eta_n = \xi_n^{(1)} - \xi_n^{(2)}$ and R_{N-k} are local multipliers of Eq. (6). Comparing this formula with Eq. (8), one can see that the only difference between them is the coefficients of the (same) local multipliers R_{N-k}. For the case of parametric noise, the coefficients $\eta_{k-1} f_a(x_{k-1}^*, a)$ are also weakly correlated random numbers, because the synchronous trajectory $\{x_n^*\}$ on the diagonal is chaotic. The distribution density function for ηf_a is presented in Fig. 4(c). Since the values of ηf_a are bounded in the interval $[-2\sqrt{3}, 2\sqrt{3}]$, the coefficients have no effect on the unbounded growth of $S_N^{(n)}$, as in the case of additive noise. Consequently, the values of the NSE for both cases of additive and parametric noise become the same, which has also been numerically confirmed in the unidirectionally coupled case of $\alpha = 1$. In this sense, the effect of parametric noise on weak synchronization becomes the same as that of the additive noise.

So far, we have investigated the noise effect in the unidirectionally coupled case with the asymmetry parameter $\alpha = 1$. Through Eq. (4), one can easily see that the NSE for a given (a, c) in the case of $\alpha = 1$ is the same as that for the value of $[a, c/(2-\alpha)]$ in other coupled 1D maps with $0 \leqslant \alpha < 1$ in Eq. (1). Thus, the results of the NSEs given in Fig. 3(b) may be converted into those for the case of general α only by a scale change in the coupling parameter such that $c \to c/(2-\alpha)$. For this case, the bubbling regime for the case of $\alpha = 1$ is always transformed into a bubbling regime for any other value of α. However, the riddling regime for the case of $\alpha = 1$ is transformed into a bubbling or riddling regime depending on the value of α. For more details on the effect of asymmetry, refer to Ref. [12].

III. CHARACTERIZATION OF THE AVERAGE INTERBURST TIME AND THE AVERAGE LIFETIME OF CHAOTIC TRANSIENT

In this section, in terms of the NSEs we characterize the noise effect on the power-law scaling behavior of the average time spent near the diagonal for the bubbling and riddling cases. The scaling exponent for such average characteristic time is found to be given by the reciprocal of the NSE, as in the parameter-mismatching case. Consequently, both the noise and the parameter mismatch have essentially the same effect on the scaling behavior of the average characteristic time.

As an example, we consider the effect of additive noise on both the bubbling and the riddling occurring in the regime of weak synchronization for $a = 1.82$ in the unidirectionally coupled case of $\alpha = 1$. In the presence of noise, the weakly stable SCA is transformed into a bubbling attractor or a chaotic transient, depending on the global dynamics. For this case the quantity of interest is the average time τ spent near the diagonal. For the case of the bubbling attractor, τ is the average interburst time, while for the case of the chaotic transient, τ is its average lifetime. As c is varied from the bubbling or riddling transition point, τ becomes short because the strength of local transverse repulsion of periodic repellers embedded in the SCA increases.

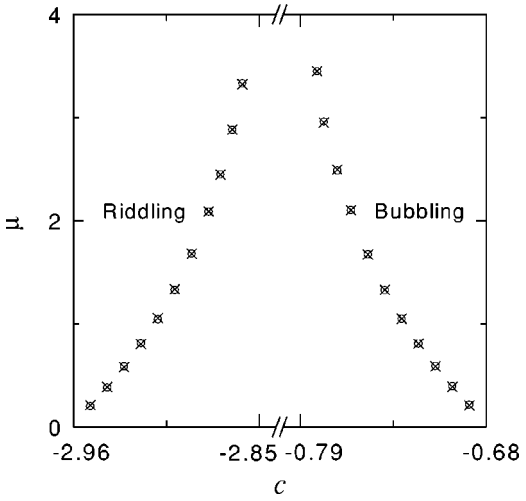

FIG. 5. (a) Plot of the scaling exponents μ (open circles) for the average characteristic time (i.e., average interburst time for the bubbling case and average chaotic transient lifetime for the riddling case) versus c in the case of additive noise when $\alpha = 1$ and $a = 1.82$. They agree well with the reciprocals of the NSEs (crosses).

For the case of bubbling, the bubbling attractor is in the laminar phase when the magnitude of the deviation from the diagonal is less than a threshold value u_b^* (i.e., $|u_n| < u_b^*$). Otherwise, it is in the bursting phase. Here u_b^* is very small compared to the maximum bursting amplitude. For each c, we follow the trajectory starting from the initial condition (0,0) until 50 000 laminar phases are obtained, and then we get the average laminar length τ (i.e., the average interburst time) that scales with σ as [21]

$$\tau \sim \sigma^{-\mu}. \tag{16}$$

The plot of the scaling exponent μ (denoted by circles) versus c is shown in Fig. 5. As c increases toward the blow-out bifurcation point, the value of μ decreases, because the average laminar length shortens.

For each c in the regime of riddling, we consider an ensemble of trajectories starting from 1000 initial points randomly chosen with uniform probability in the range of $x \in (1-a, 1)$ on the diagonal, and obtain the average lifetime of the chaotic transients. A trajectory may be regarded as having escaped once the magnitude of deviation u_n from the diagonal becomes larger than a threshold value u_c^* such that an orbit point with $|u| > u_c^*$ lies sufficiently outside the basin of the SCA. Thus, the average lifetime τ is found to scale with σ as [21]

$$\tau \sim \sigma^{-\mu}. \tag{17}$$

The plot of the scaling exponent μ (denoted by circles) versus c is given in Fig. 5. As c decreases toward the blow-out bifurcation point, the average lifetime shortens, and hence the value of μ decreases.

We note that the scaling exponent μ is associated with the NSE δ as follows. For a given σ, consider a trajectory starting from a randomly chosen initial orbit point on the diagonal. Then, From Eq. (11) the average characteristic time τ at which the magnitude of the deviation from the diagonal becomes the threshold value $u_{b,c}^{*}$ can be obtained:

$$\tau \sim \sigma^{-1/\delta}. \tag{18}$$

Hence the scaling exponent μ for τ is given by the reciprocal of the NSE δ,

$$\mu = 1/\delta. \tag{19}$$

The reciprocal values of δ (denoted by crosses) are also plotted in Fig. 5, and they agree well with the values of μ (denoted by circles). This reciprocal relation has also been confirmed for the case of parametric noise. Furthermore, the same reciprocal relation between the scaling exponent for τ and the parameter-sensitivity exponent exists also in the parameter-mismatching case [18]. Thus the scaling exponents for τ in both cases of noise and parameter mismatch also become the same [21], because the values of the NSE and the parameter sensitivity exponent are the same. Hence the noise and parameter mismatch have the same effect on the power-law scaling behavior of the average characteristic time τ.

IV. SUMMARY

We have studied the effect of additive and parametric noise on weak synchronization in coupled identical 1D maps. Because of the existence of positive local transverse Lyapunov exponents, the weakly stable SCA becomes sensitive with respect to the variation of noise strength. To measure the degree of such noise sensitivity, we have introduced a quantifier, called the NSE, and quantitatively characterized the noise sensitivity of the weakly stable SCA for both the bubbling and riddling cases occurring in the regime of weak synchronization. For the case of bounded noise, the values of the NSE have been found to become the same as those of the parameter sensitivity exponent, independently of whether the noise is additive or parametric. In terms of these NSEs, we have also characterized the noise effect on the power-law scaling of the average interburst time and the average lifetime of chaotic transient. It has thus been found that the scaling exponent for the average characteristic time and the NSE have the same reciprocal relation as in the parameter-mismatching case. Consequently, the noise and the parameter mismatch have basically the same effect on the power-law scaling behavior of the average characteristic time. Finally, we expect that the method of characterizing the noise sensitivity of the weakly stable SCA in terms of the NSE may be generalized to the coupled systems consisting of the high-dimensional maps such as the Hénon map or the oscillators.

ACKNOWLEDGMENTS

S.Y.K. thanks Professor Ott for hospitality and support during his visit to the University of Maryland. This work was supported by the Korea Research Foundation (Grant No. KRF-2001-013-D00014). A.J. and S.P.K. acknowledge support from the Russian Foundation for Basic Research (Grant No. 00-02-17509) and CRDF (Grant No.0 REC-006).

[1] H. Fujisaka and T. Yamada, Prog. Theor. Phys. **69**, 32 (1983).
[2] A.S. Pikovsky, Z. Phys. B: Condens. Matter **50**, 149 (1984).
[3] V.S. Afraimovich, N.N. Verichev, and M.I. Rabinovich, Radiophys. Quantum Electron. **29**, 795 (1986).
[4] L.M. Pecora and T.L. Carroll, Phys. Rev. Lett. **64**, 821 (1990).
[5] K.M. Cuomo and A.V. Oppenheim, Phys. Rev. Lett. **71**, 65 (1993); L. Kocarev, K.S. Halle, K. Eckert, L.O. Chua, and U. Parlitz, Int. J. Bifurcation Chaos Appl. Sci. Eng. **2**, 973 (1992); L. Kocarev and U. Parlitz, Phys. Rev. Lett. **74**, 5028 (1995); N.F. Rulkov, Chaos **6**, 262 (1996).
[6] P. Ashwin, J. Buescu, and I. Stewart, Nonlinearity **9**, 703 (1996).
[7] Y.-C. Lai, C. Grebogi, J.A. Yorke, and S.C. Venkataramani, Phys. Rev. Lett. **77**, 55 (1996).
[8] V. Astakhov, A. Shabunin, T. Kapitaniak, and V. Anishchenko, Phys. Rev. Lett. **79**, 1014 (1997); V. Ashtakhov, M. Hasler, T. Kapitaniak, V. Shabunin, and V. Anishchenko, Phys. Rev. E **58**, 5620 (1998).
[9] Yu.L. Maistrenko, V.L. Maistrenko, O. Popovich, and E. Mosekilde, Phys. Rev. E **57**, 2713 (1998); **60**, 2817 (1999); O. Popovych, Yu.L. Maistrenko, E. Moskilde, A. Pikovsky, and J. Kurths, Phys. Lett. A **275**, 401 (2000); Phys. Rev. E **63**, 036201 (2001).
[10] Yu.L. Maistrenko, V.L. Maistrenko, A. Popovich, and E. Mosekilde, Phys. Rev. Lett. **80**, 1638 (1998); G.-I. Bischi and L. Gardini, Phys. Rev. E **58**, 5710 (1998).
[11] S.-Y. Kim and W. Lim, Phys. Rev. E **63**, 026217 (2001); S.-Y. Kim, W. Lim, and Y. Kim, Prog. Theor. Phys. **105**, 187 (2001).
[12] S.-Y. Kim and W. Lim, Phys. Rev. E **64**, 016211 (2001).
[13] C. Mira, L. Gardini, A. Barugola, and J.-C. Cathala, *Chaotic Dynamics in Two-Dimensional Noninvertible Maps* (World Scientific, Singapore, 1996); R.H. Abraham, L. Gardini, and C. Mira, *Chaos in Discrete Dynamical Systems* (Springer, New York, 1997).
[14] P. Ashwin, J. Buescu, and I. Stewart, Phys. Lett. A **193**, 126 (1994); J.F. Heagy, T.L. Carroll, and L.M. Pecora, Phys. Rev. E **52**, 1253 (1995); S.C. Venkataramani, B.R. Hunt, E. Ott, D.J. Gauthier, and J.C. Bienfang, Phys. Rev. Lett. **77**, 5361 (1996).
[15] S.C. Venkataramani, B.R. Hunt, and E. Ott, Phys. Rev. E **54**, 1346 (1996).

[16] J.C. Alexander, J.A. Yorke, Z. You, and I. Kan, Int. J. Bifurcation Chaos Appl. Sci. Eng. **2**, 795 (1992); E. Ott, J.C. Sommerer, J.C. Alexander, I. Kan, and J.A. Yorke, Phys. Rev. Lett. **71**, 4134 (1993); J.C. Sommerer and E. Ott, Nature (London) **365**, 136 (1993); E. Ott, J.C. Alexander, I. Kan, J.C. Sommerer, and J.A. Yorke, Physica D **76**, 384 (1994); J.F. Heagy, T.L. Carroll, and L.M. Pecora, Phys. Rev. Lett. **73**, 3528 (1994).

[17] A. Pikovsky and U. Feudel, Chaos **5**, 253 (1995).

[18] A. Jalnine and S.-Y. Kim, Phys. Rev. E **65**, 026210 (2002).

[19] E. Ott and J.C. Sommerer, Phys. Lett. A **188**, 39 (1994); Y. Nagai and Y.-C. Lai, Phys. Rev. E **56**, 4031 (1997).

[20] S.-Y. Kim and H. Kook, Phys. Rev. E **48**, 785 (1993).

[21] S.-Y. Kim, W. Lim, and Y. Kim, Prog. Theor. Phys. **107**, 239 (2002).